

Time resolved study of femtosecond laser induced micro-modifications inside transparent brittle materials

F. Hendricks^{a,*}, V.V. Matylitsky^a, M. Domke^b, Heinz P. Huber^c

^a*Spectra-Physics, Feldgut 9, 6830 Rankweil, Austria*

^b*Vorarlberg University of Applied Sciences - Josef Ressel Center for material processing with ultrashort pulsed lasers, Hochschulstraße 1, 6850 Dornbirn, Austria*

^c*Laser Center of Munich University of Applied Sciences, Lothstrasse 34, 80335 München, Germany*

Abstract

Non-ablative methods for cutting of transparent, brittle materials, like the newly developed femtosecond laser process ClearShape™ from Spectra-Physics®, are based on producing a micron-sized material modification track with well-defined geometry inside the material. The key point for further improvement of the process is to understand the induced modification by a single femtosecond laser shot. In this work, pump-probe microscopy techniques have been applied to study the defect formation inside of transparent materials on a time scale between one nanosecond to several tens of microseconds. The observed effects include longitudinal and transversal acoustic wave propagation as well as mechanical stress formation in the bulk of the glass. The enhancement of the lateral defect length by temporal laser burst mode is explained. Besides of better understanding of underlying physical mechanisms, our experimental observations have helped us to find optimal process parameters for the ClearShape™ glass cutting process.

© 2016 The Authors. Published by Bayerisches Laserzentrum GmbH

Keywords: Femtosecond; micromachining; glass; time-resolved; pump-probe microscopy; bulk modification; dielectrics; laser; burst

1. Introduction

Optically transparent materials like glasses and sapphire are commonly used in various manufacturing sectors ranging from consumer electronics, automotive applications, medical device manufacturing and solar industry to semiconductor for substrates, like sapphire for LED manufacturing. For standard glasses, which are used for example in the building industry, mechanical separation methods like diamond scribing and breaking offer sufficient quality and speed. However, new generation glasses, such as chemically strengthened glass substrates, require new processing methods. There is also an increasing trend to thinner glasses below 1 mm thickness and even below 0.1 mm thickness. Mechanical methods struggle here not only because of the machining process itself, but also because there are always micro-cracks present after processing which lead to very low quality and an increased risk of breaking of the machined part. The consumer electronics industry is one of the main driving markets for this new generation of chemically strengthened and thin glasses, since these devices need to be lightweight and robust for everyday use. Lasers offer an interesting alternative to conventional processing methods, because they allow machining with higher quality and speed, and requiring no or only minor post-processing. In particular, ultrashort pulsed lasers in the picosecond and femtosecond time regime provide certain advantages in comparison with longer pulsed lasers for the machining of transparent material (Chichkov et al., 1996; Chien and Gupta, 2004; Momma et al., 1996). The absorption process for ultrashort pulsed lasers is a strongly non-linear process. Because of that, it is possible to machine materials which are transparent for the laser wavelength, and there is no need to use high power UV or far-IR lasers. When an ultrashort laser pulse is focused inside glass, only the localized region in the neighborhood of the focal volume absorbs laser energy. Therefore, the processing volume is strongly defined. This allows extremely defined machining with no heat affected zone and, what is especially important for glass substrates, with no micro-cracks or chipping on the

* Corresponding author. Tel.: +43-5522-82646-183; fax: +43-5522-82646-800 .
E-mail address: frank.hendricks@spectra-physics.at

surface. Besides surface ablation processes, it is also possible to induce localized and defined micro-defects in the bulk of a transparent material without affecting the surface. These defects can be used for controlled crack propagation and separation of the workpiece. This work focuses on the creation and analysis of a single micro-defect induced in soda-lime glass by a burst of several femtosecond laser pulses. The analysis comprises the dynamics of the laser-matter interaction by time-resolved pump-probe microscopy technique.

2. Laser system

The experiments in this work have been performed with a commercially available Spirit[®] laser from Spectra-Physics. This laser source has a wavelength of 1040 nm, average output power up to 16 W and pulse durations of 350 femtoseconds. The basic repetition rate can be divided by any integer value with an integrated acousto-optic-modulator, which also can be used to attenuate the maximum available pulse energy of 120 μ J. A special feature of the Spirit laser is the burst mode operation in a regenerative amplifier as illustrated in Figure 1. The femtosecond pulses are supplied in a burst train which contains several pulses. The time spacing between the pulses in one burst is around 13 ns. The number of pulses in one burst and the intensity profile can be controlled. The time spacing between two consecutive bursts is determined by the repetition rate of the laser. The contained energy in one burst is constant, no matter if a single pulse is set or multiple pulses are defined in the user-controlled software.

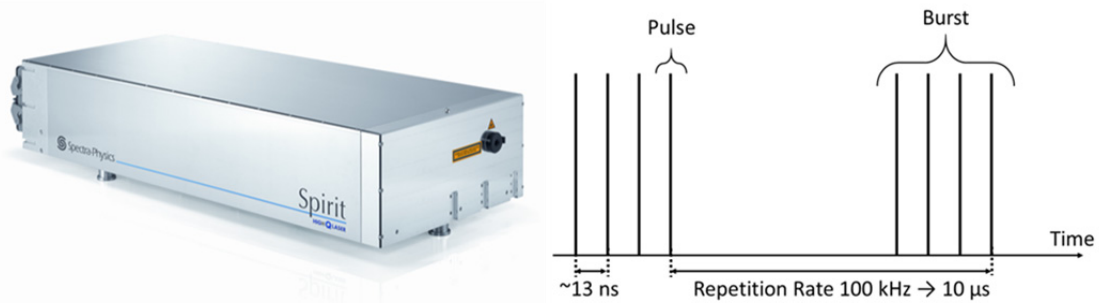


Fig. 1. The left image shows Spirit femtosecond laser from Spectra-Physics. On the right, the burst mode operation with 4 pulses in one burst separated by ~ 13 ns and supplied with basic repetition rate of 100 kHz is illustrated.

3. Time resolved study

The timescale of the energy transfer from electrons to the lattice has been determined to be around 10-15 ps, and the hydrodynamic motion and void formation has an estimated time of a few up to one hundred nanoseconds (Eaton et al., 2012; Gamaly, 2011). These fast processes cannot be studied using commercially available high speed cameras because the shutter speed is usually in the microsecond time regime. A completely different approach to resolve ultrafast processes is time-resolved pump-probe microscopy. This technique assumes that the material is homogenous and each laser pulse has the same properties. Therefore the material reaction to each pulse is the same. The exposure time for a detector used in the pump-probe microscopy technique is determined by the probe pulse length of the used laser which acts as the illumination light source. The material reaction to the pump pulse is recorded at different time delays at different positions on the sample. The time delay between the probe and pump pulses sets the point of time which is recorded. The temporal resolution is defined by the pulse duration of the probe laser. Since the timescale of interest ranges into the microsecond time regime, using only one laser for pumping and probing by an optical delay line, is not suitable, because the delay line would be very long. Therefore, a second laser source is used for probing, which must be synchronized with the pump laser as described in (Domke et al., 2012).

3.1. Experimental setup

The pump-probe microscopy setup is shown in Figure 2. The initiated process is probed in transmission mode, which is more suitable for observing transmission changes in the bulk of transparent materials, compared to reflective approaches. The femtosecond pump pulse is emitted from the Spirit laser. An active Q-switched Nd:YVO₄ laser source (wavelength 532 nm, pulse duration 600 ps) has been used as a probe laser. The delay time for the probe pulse with respect to the pump pulse can be set by the digital delay generator. For synchronization of the time-resolved setup, the gate signal from the Pockels cell of the Spirit laser is used. The Spirit acts as a master to which the ps-laser output is synchronized. An acousto-optic-modulator (AOM), which is also controlled by the digital delay generator, acts as fast shutter in order to control the emission of exactly one

pulse from the Spirit laser. The time delay of the ps-laser pulse (pump) with respect to the Spirit pulse (probe) can be set to maximum of 2000 seconds with an electronic jitter of approximately 200 ps.

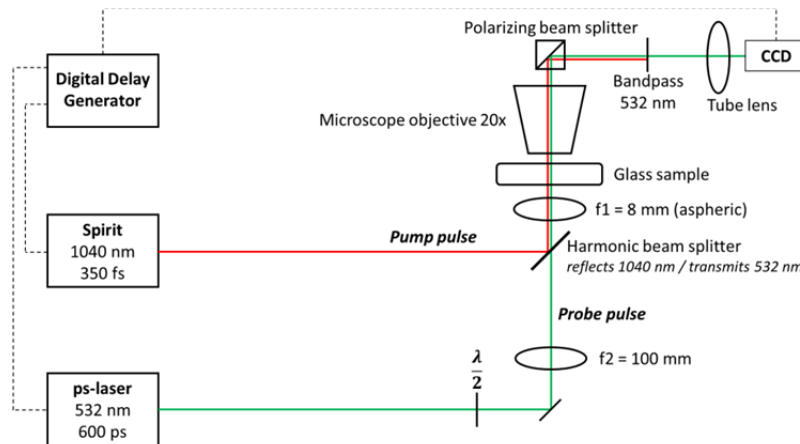


Fig. 2. Schematic illustration of the used pump-probe microscope in transmission configuration. For nanosecond resolution measurements the picosecond laser with wavelength of 532 nm and pulse length of around 600 ps has been used for probing.

The pump pulse and the probe pulse were superimposed locally by a harmonic beam splitter, which reflects the 1040 nm wavelength of the pump pulse and transmits the 532 nm wavelength of the probe pulse. The lenses f_1 and f_2 form a Kepler type telescope to achieve homogeneous and collimated illumination with the appropriate spot size in the sample. The pump pulse is focused approximately $500 \mu\text{m}$ below the entrance surface of the soda-lime glass sample (thickness 1 mm) by an aspheric lens f_1 (NA 0.5, focal length 8 mm). The process is observed with a 20x microscope objective (NA 0.29). A bandpass filter blocks the pump pulse and shields the CCD camera from ambient light. A tube lens focuses the light on the 14 bit CCD camera. The exposure time of the camera is $5 \mu\text{s}$. The rotatable half-wave plate in the probe path before the sample and the polarizing beam splitter before the tube lens form a polariscope-like configuration and can be used to analyze stress induced birefringence in the sample. To improve image quality and obtain quantitative results, image processing techniques have been applied to the raw bitmap images. Effects that reduce the image quality are material inhomogeneity, contamination by particles on the sample and pulse fluctuation of the probe pulse. To minimize influences of these effects on the measured signal, difference images have been calculated. For each laser shot, an additional image has been acquired 1 second before the excitation by the pump pulse. The additional image is subtracted from the image acquired at the delay time. By means of this technique, background noise can be reduced and the relative transmission change $\Delta T/T$ caused by the laser induced material change modification can be observed more clearly with a resolution $\Delta T/T$ of approximately 1% (Domke et al., 2012).

3.2. Results and discussion

Figure 3 shows the comparison of single spot modifications in soda lime glass using a circular and an elliptical laser beam. The applied energy per shot is $32 \mu\text{J}$. In both cases, the induced modifications contain a central circular void with diameter of approximately $4 \mu\text{m}$.

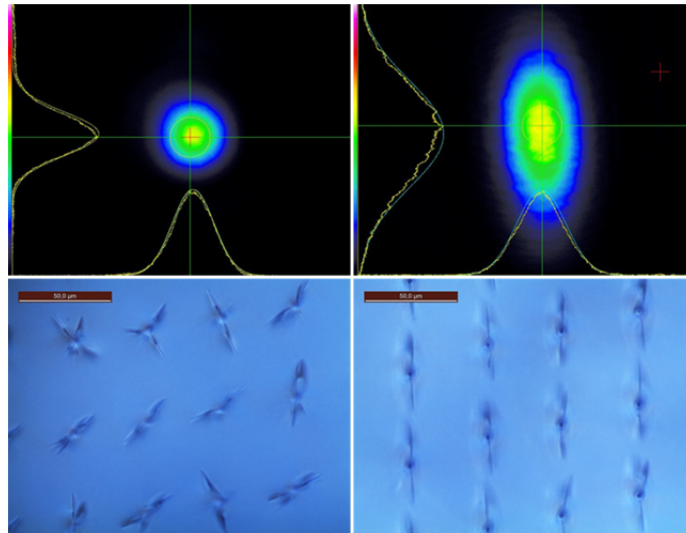


Fig. 3. Comparison of circular and elliptical beam shape. Beam profile is measured before focusing lens. The microscope images compare the lateral shape of the induced modifications for circular and elliptical beam shape.

The void is surrounded by densified material as proposed and investigated by (Gamaly, 2011; Gamaly et al., 2006). The void formation and densification is commonly understood in the following way: The laser energy is absorbed by non-linear absorption and the electrons transfer their energy to the lattice. The lattice is heated on an ultrafast time scale, melting and probably evaporation as well as plasma formation is the consequence. A supersonic shockwave is generated, which is damped to a propagating sound wave, transporting the energy away from the deposition area. The plasma expansion together with the high pressure pushes the material out of the center which leads to the formation of the void and the densification of the surrounding material. The majority of the laser energy is dissipated in the material until the shockwave stops and transforms into an acoustic pressure wave, which propagates further into the material but makes no permanent material modification. For higher energy doses, starting from the densified area, a crack or multiple cracks are formed. While the crack shape and orientation is not very defined for the circular case, using an elliptical beam allows producing linear defined cracks with a controlled direction and only minor side-cracks. From shot to shot, the orientation of the crack is not changing, which is crucial for the pump-probe microscopy technique, because the same material response of each shot is assumed. The crack growth can be explained by tensile stresses at the border of the densified area. For the circular case, the tensile stress is homogeneously distributed around the densification zone and the crack has no preferred direction. For an elliptically shaped laser beam, there is a tensile stress concentration at the small radii of the ellipse and therefore the crack growth direction is defined.

When the pulses are delivered in a burst train with a temporal pulse separation of ~ 13 ns each succeeding pulse hits pre-excited material and can use this excitation state for further modification in an accumulative process. The burst with the pulse separation of ~ 13 ns leads to a partial delivery of the energy in the material. The work against the material strength is not done by a single pulse with much energy, but more in a portion-wise energy delivery. This finally leads to longer cracks and a more defined crack shape. For time-resolved analysis of the burst mode influence the described pump-probe microscopy setup has been used. Since the most interesting effects happen from zero to 100 ns, the delay time step has been set to 1 ns in this region. From 100 to 200 ns, a step of 5 ns has been chosen. For observations up to 100 μs the delay time step has been increased with a kind of logarithmic increment. The results reveal that after the first pulse of the burst only a void appears without visible crack formation (see Figure 4, 6 ns). Starting from the void as a center, a wave propagates into the surrounding material without causing a permanent material change. After this first wave, a second wave starts propagating with similar shape, lower intensity and slower velocity of the wave front. That means that each pulse causes two waves. The second pulse in the burst results in a little crack slightly bigger than the void diameter. In Figure 4 after 29 ns the void and the crack can be observed. Additionally, the first and second waves, which belong to the second pulse in the burst, can be seen. From 29 ns up to 37 ns the effect of the third pulse can be studied. At 30 ns the first wave starts propagating away from the void. The crack length increases along with the propagation of the second wave front (32-34 ns). After 37 ns the crack increase from the third pulse is finished and the second wave propagates further into the surrounding material without any material change. Each laser pulse, from pulse two to pulse nine, increases the crack length step by step up to a final crack length of around 50 μm .

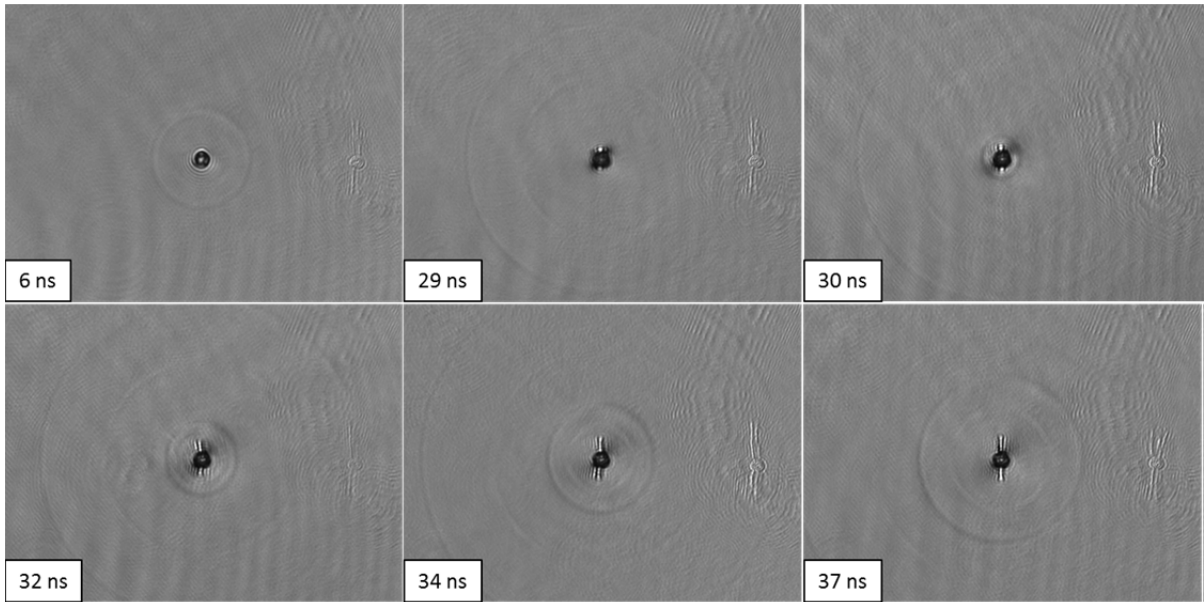


Fig. 4. Time series of induced modification in soda-lime glass. From 29 ns to 37 ns the increase of the lateral crack size caused by the third pulse in the burst is shown. The artefact right of the defect is from the previously produced crack step. Artefact distance of $\sim 100 \mu\text{m}$ can be used as scale.

The obtained datasets can be analyzed by plotting a cross-section of the normalized transmission signal $\Delta T/T$ depending on the delay time along a desired line in the time resolved 2D microscope pictures. For investigation of the crack formation the cross-section line has been set vertically, i.e. along of the direction of the crack formation (Figure 5). It can be seen that the crack length increases stepwise with each pulse in the burst. The first pulse (0 ns) causes only void formation and no crack. The minor crack formation of the second pulse cannot be seen in this image because the crack size is only slightly bigger than the void. The first major crack increase starts with the third pulse of the burst. The time step of the crack increase corresponds well with the time of ~ 13 ns between two consecutive pulses.

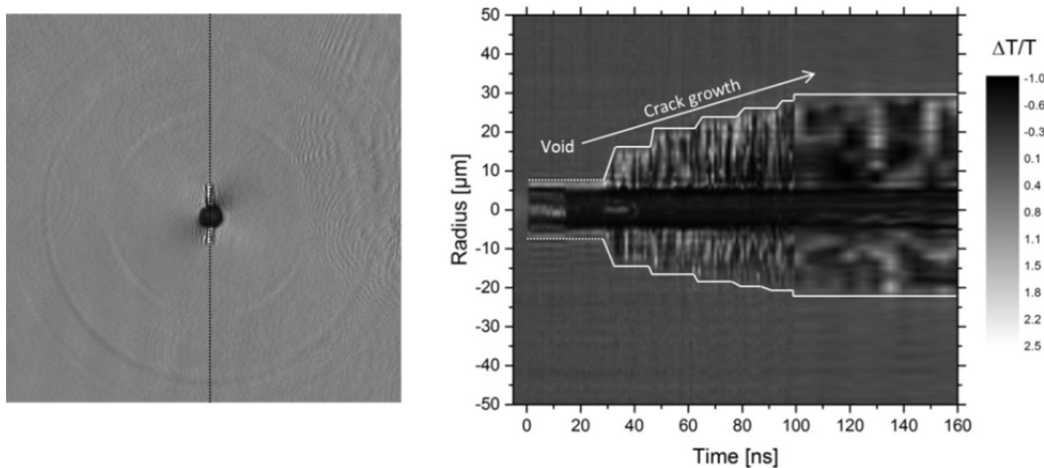


Fig. 5. Time-resolved normalized transmission signal along the cross-section line defined in the left image.

The wave front radius shows a linear time dependence and the slope, which characterizes the wave velocity, can be obtained from a linear fit (see Figure 6). The measurements reveal that the first wave front has a velocity of around $5.9 \mu\text{m/ns}$ and the second wave travels with a speed of approximately $3.5 \mu\text{m/ns}$. From these values it can be concluded that the first wave is a longitudinal acoustic wave and the second one is a transversal shear wave, because the velocities correspond well with the reported acoustic wave velocities for soda-lime glass (longitudinal wave: $6 \mu\text{m/ns}$; shear wave: $3.2 \mu\text{m/ns}$; (Maev, 2013)). Shear waves in the acoustic theory have always a slower travel velocity than the longitudinal waves and less intensity. The shear waves induce mechanical shear stress perpendicular to the propagation direction. Therefore the crack increase caused by each pulse in the burst can be explained by the tensile stresses induced by the shear wave. The wave needs to travel first from its origin in the center to the crack tips. The tensile stresses increase the crack as the wave travels

outside of the center of symmetry. When the energy is no longer sufficient to overcome material strength, the crack growth by this pulse is completed and the wave travels further without permanent material change.

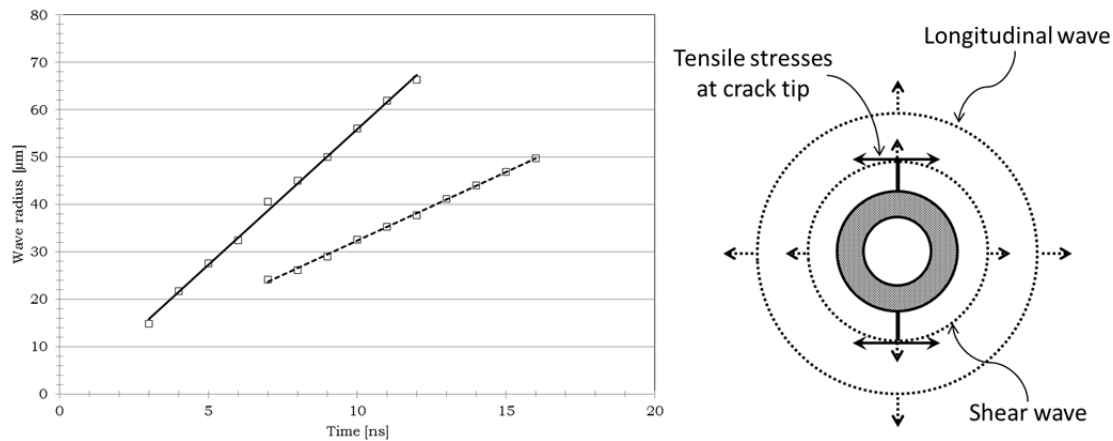


Fig. 6. (left) Wave radii and fitted wave velocity for longitudinal wave (solid line, $5.8 \mu\text{m/ns}$) and transversal shear wave (dashed line, $3.4 \mu\text{m/ns}$). (Right) Schematic illustration of wave propagation and their impact on crack growth.

4. Summary

In summary, the crack generation in the bulk of soda-lime glass by femtosecond laser pulses with pulse energies up to $32 \mu\text{J}$ supplied by a burst train consisting of several pulses separated by around 13 ns , can be understood in the following way: The first pulse induces a void surrounded by densified material. Tensile mechanical stresses at the border between the densified and not-affected area induce an initial seed crack. Each pulse in the burst creates two waves. From the wave speeds it can be concluded that the first wave is a longitudinal acoustic wave ($5.9 \mu\text{m/ns}$) and the second wave is a transversal shear acoustic wave ($3.5 \mu\text{m/ns}$). The shear wave of the second and each subsequent pulse travels from the center of symmetry to the crack tips, where the tensile stresses, which are perpendicular to the propagation direction, increase the crack length as the shear wave propagates (Sakakura, 2014; Sakakura et al., 2011). The shear wave loses energy, the crack stops increasing and the wave travels further into the volume without material modifications. The crack is increased stepwise from each pulse until the pulse energy is no longer sufficient to overcome the material strength and the crack length is not increased further. Using an overall burst energy of $32 \mu\text{J}$ and approximately 10 pulses separated by $\sim 13 \text{ ns}$, an overall crack length (tip to tip) of $50 \mu\text{m}$ can be achieved. The perfectly clear and straight shape of the induced cracks makes them an ideal tool for cutting applications, like the non-ablative patent-pending ClearShape™ process (“ClearShape industrial laser cutting process,” n.d.) developed by Spectra-Physics. The absence of any side-cracks into the surrounding material is a crucial characteristic for the achievable high strength and quality. The increased lateral crack length of up to $50 \mu\text{m}$ leads also to higher processing speeds, since the modification spots can have larger separation distances and the scanning speed can be increased. For example, using a 4 W average power laser system with a repetition rate of 100 kHz the maximum translation speed can be set up to 5 m/s .

References

- Chichkov, B.N., Momma, C., Nolte, S., Alvensleben, F. von, Tünnermann, A., 1996. Femtosecond, picosecond and nanosecond laser ablation of solids. *Appl. Phys. A* 63, 109–115. doi:10.1007/BF01567637.
- Chien, C.Y., Gupta, M.C., 2004. Pulse width effect in ultrafast laser processing of materials. *Appl. Phys. A* 81, 1257–1263. doi:10.1007/s00339-004-2989-z.
- ClearShape industrial laser cutting process [WWW Document], n.d. URL <http://www.spectra-physics.com/clearshape>
- Domke, M., Rapp, S., Schmidt, M., Huber, H.P., 2012. Ultrafast pump-probe microscopy with high temporal dynamic range. *Opt. Express* 20, 10330–10338.
- Eaton, S.M., Cerullo, G., Osellame, R., 2012. Fundamentals of Femtosecond Laser Modification of Bulk Dielectrics, in: Osellame, R., Cerullo, G., Ramponi, R. (Eds.), *Femtosecond Laser Micromachining, Topics in Applied Physics*. Springer Berlin Heidelberg, pp. 3–18.
- Gamaly, E., 2011. *Femtosecond laser-matter interactions: theory, experiments and applications*. Pan Stanford Publishing, Singapore.
- Gamaly, E.G., Juodkazis, S., Nishimura, K., Misawa, H., Luther-Davies, B., Hallo, L., Nicolai, P., Tikhonchuk, V.T., 2006. Laser-matter interaction in the bulk of a transparent solid: Confined microexplosion and void formation. *Phys. Rev. B* 73, 214101. doi:10.1103/PhysRevB.73.214101.
- Maev, R.G., 2013. *Advances in Acoustic Microscopy and High Resolution Imaging: From Principles to Applications*. John Wiley & Sons.
- Momma, C., Chichkov, B.N., Nolte, S., von Alvensleben, F., Tünnermann, A., Welling, H., Wellegehausen, B., 1996. Short-pulse laser ablation of solid targets. *Opt. Commun.* 129, 134–142. doi:10.1016/0030-4018(96)00250-7.

- Sakakura, M., 2014. Modulation of Crack Generation inside a LiF Single Crystal by Interference of Laser Induced Stress Waves. *J. Laser MicroNanoengineering* 9, 15–18. doi:10.2961/jlmn.2014.01.0004.
- Sakakura, M., Tochio, T., Eida, M., Shimotsuma, Y., Kanehira, S., Nishi, M., Miura, K., Hirao, K., 2011. Observation of laser-induced stress waves and mechanism of structural changes inside rock-salt crystals. *Opt. Express* 19, 17780–17789.